Two-Inch High Quality Diamond Heteroepitaxial Growth on Sapphire for Power Devices

Seong-Woo Kim[1)*], Makoto Kasu[2)]

1) Adamant Namiki Precision Jewel Co., Ltd. 3-8-22 Shinden, Adachi-ku, Tokyo, 123-8511 Japan, s-kim@ad-na.com, +81-3-3919-0101.
2) Department of Electrical and Electronic Engineering, Saga University, 1 Honjomachi, Saga, 840-8502 Japan.

Keywords: … Heteroepitaxial diamond, large area, high quality, step flow growth, sapphire , MOSFET

Abstract

Two-inch-diameter high-quality free-standing (001) diamond layers were grown on misoriented (11 $\bar{2}$ 0) sapphire. The substrate misorientation allows step-flow growth, and tensile stress is released in the diamond layer. Consequently, the diamond layer delaminates naturally from the substrate without cracking. For the diamond grown on the sapphire misoriented by 7° toward the [1$\bar{1}$00] direction, the widths of the (004) and (311) X-ray rocking curves were 98.35 and 175.3 arcsec, respectively, the lowest ever reported. The curvature radius of the diamond was 99.64 cm in the [1$\bar{1}$00] direction and 260.21 cm in the [0001] direction of the substrate, the highest ever reported. We also demonstrated diamond metal oxide semiconductor field effect transistors (MOSFETs) on high-quality heteroepitaxial diamond (Kenzan Diamond^{TM}) with NO_2 p-type doping and an Al_2O_3 passivation overlayer, which exhibited a high off-state breakdown voltage of −2608 V. The MOSFET showed a specific on-resistance of 19.74 mΩ·cm^2 and a maximum drain current density of −288 mA/mm, with an extremely low gate leakage current <10^{-6} mA/mm. The Baliga's Figure-Of-Merits was experimentally determined to be 344.6 MW/cm^2, and the maximum DC power density was observed to be 21.0 W/mm.

Diamond power semiconductor devices exhibit characteristics beyond those of SiC and GaN.[1,2)] This is because the diamond possesses exceptional physical properties, such as high breakdown electric field (>10 MV cm^{-1}), extremely high thermal conductivity (22 Wcm^{-1}K^{-1}),[3)] and high carrier mobility (4500 and 3800 cm^2 V^{-1} s^{-1} for electrons and holes, respectively).[4)]

For semiconductor device research and development in corporate laboratories, a high-quality 2 inch diameter wafer is essential. However, the size of commercially available single crystal diamond grown by high-pressure high-temperature method is 4 ×4 mm^2. Therefore, diamond heteroepitaxial growth has been extensively studied for several decades.[5-7)]

In this paper, we demonstrated a 2 inch diameter high quality free-standing (001) diamond layer grown on a sapphire misoriented (11$\bar{2}$0) A-plane substrate in step-flow mode. Using the misoriented sapphire substrate, step-flow growth in diamond is realized, the tensile stress in the diamond layer is released, the curvature radius increases (bending reduces), and the diamond layer delaminates naturally from the substrate without the microneedle technique, and without cracking. We also demonstrated an FET fabricated on our grown heteroepitaxial diamonds, KENZAN Diamond^{TM}.

Figure 1 shows the fabrication procedure for free-standing heteroepitaxial diamond grown on Ir/misoriented sapphire. The growth parameters were described in Ref. 8. First, a sapphire (α-Al_2O_3) (11$\bar{2}$0) misoriented substrate was prepared [**Fig. 1(a)**]. The misorientation angle was changed from 0 to 7°, and the misorientation direction was the [1 $\bar{1}$ 00] m-direction or [0001] c-direction. Then, an approximately 1 μm thick Ir buffer layer was deposited on the sapphire substrate using a sputtering method. As shown in **Fig. 1(b)**, a bias-enhanced nucleation (BEN)[9)] for diamond nucleation was performed on the Ir buffer layer using DC plasma CVD.

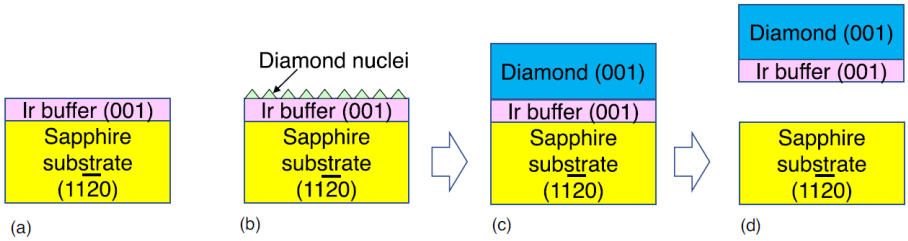

Fig. 1. Fabrication procedure of heteroepitaxial diamond on Ir buffer/sapphire. (a) Ir buffer deposition on misoriented sapphire (11$\bar{2}$0), (b) diamond BEN, (c) diamond growth on Ir/sapphire, (d) diamond delamination.

H_2-diluted CH_4 was used as the gas source. Here, the substrate was negatively biased so that positively charged CH_3 radicals with kinetic energy were bombarded onto the Ir surface promoting diamond nucleation. As shown in **Fig. 1(c)**, the diamond layer was grown on the BEN-treated Ir buffer. The $CH_4/(CH_4 + H_2)$ gas ratio was 5.5%. The substrate temperature was set to 1000 °C. N_2 gas was slightly added. The diamond growth rate was 16.5 μmh^{-1}. The grown diamond thickness was in the range of 800– 1000 µm. Owing to the misoriented substrate, the diamond growth proceeds in the step-flow mode. This leads to a decrease in residual stress in the diamond layer. Unlike diamond growth on a just-oriented sapphire substrate reported previously,[8] in this process, we did not use vertically aligned pillars, so-called microneedles (KENZAN), for delamination of the diamond layer from the substrate. Thus, as shown in **Fig. 1(d)**, because the coefficient of thermal expansion (CTE) of sapphire is much higher than that of diamond, during cooling the sapphire substrate contracts more than the grown diamond layer; consequently, the diamond layer with the Ir buffer layer is naturally delaminated from the sapphire substrate without any cracking. The two-column format illustrated here. To ensure proper reproducibility, uniformity, and high quality of the conference digest, the following instructions should be observed.

Figure 2 shows the epitaxial relation between diamond, Ir buffer, and sapphire substrate is determined to be diamond (001) [110]//Ir (001) [110]// sapphire (11$\bar{2}$0) [0001]. This epitaxial relation is the same as that on a just-oriented sapphire substrate.[8]

Figure 3 shows The misorientation-angle dependence of the FWHM of the XRC diamond (004) and (311) diffractions for the [0001] c- and [1$\bar{1}$00] m-misorientation directions.[10] The FWHMs for zero misorientation (just-oriented) substrate of diamond (004) and (311) were 113.4, 234.0 arcsec, respectively, where the microneedle technique was used.[8] Conversely, for the diamond without microneedle technique case, the FWHMs for zero misorientation of diamond (004) and (311) were 325– 363 and 655 arcsec, respectively. As the misorientation angle, α, increased toward either the [0001]

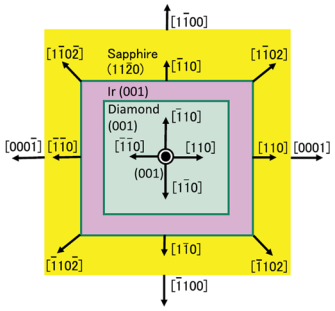

Fig. 2. Epitaxial relation of diamond, Ir, and sapphire.[8]

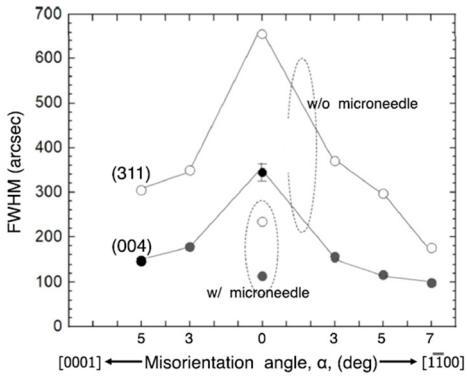

Fig. 3. Misorientation-angle dependence of the FWHM of XRC diamond (004) and (311) diffraction peaks for [0001] c- and [1$\bar{1}$00] m-misorientation directions.[10]

or [1 $\bar{1}$ 00] direction, the FWHM decreased drastically, indicating an improvement in the crystal quality. As a result, the FWHMs for α = 7° in the m-misorientation direction were the lowest. For the case of the just-oriented substrate, after diamond growth, during cooling [**Fig. 1(d)**], the sapphire substrate tended to break catastrophically because of its residual stress. However, for the case of the misoriented substrate, as the misorientation angle increased, the sapphire substrate exhibited small fractures.

Figure 4 shows the curvature of the diamond layer; thus, the diamond (004) XRC peak angle, ω, at different positions,

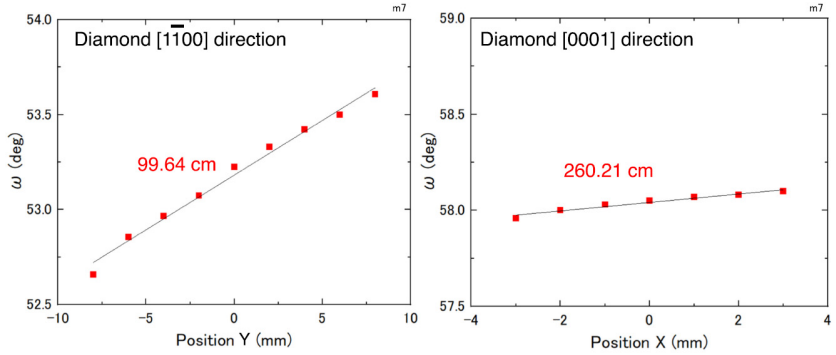

Fig. 4. Curvature of diamond layer grown on Ir (001) buffer/sapphire (11$\bar{2}$0) substrate misoriented by 7° toward the [1$\bar{1}$00] m-direction. Thus, the XRC omega angle for diamond (004) diffraction at different position. *Y* in [1$\bar{1}$00] m-direction and *X* in [0001] c-direction. The linear relation was determined by the least-square method.[10]

X, from the diamond (001) layer grown on the Ir (001) buffer/ sapphire (11 $\bar{2}$ 0) substrate misoriented by 7° toward the [1 $\bar{1}$ 00] m-direction.[10] The XRC of the (004) peak angle shifted to a higher angle. This implies that the diamond layer is convex upward, because the CTE of sapphire substrate is higher than that of the diamond layer; therefore, during cooling after diamond growth, sapphire substrate contracts more than the diamond layer. Thus, the residual stress remained after delamination. In the [1$\bar{1}$00] m-direction of the substrate, ω was 52.72126° at Y = −8.0 mm and 53.64174° at Y = 8.0 mm; by the least root-square method, the best-fitted curvature radius was determined to be 99.64 cm. Interestingly, in the [0001] direction of the substrate (perpendicular to the misorientation direction), ω was 57.97505° at X = −3.0 mm and 58.10732° at X = 3.0 mm; surprisingly, the curvature radius was determined to be 260.21 cm. This value is much longer than our previous value of approximately 90.6 cm for diamond on just-oriented substrate.[8] These results additionally support that the misorientation effect releases the tensile stress in the diamond layer.

Figure 5 shows a photograph of a 2 inch diamond freestanding heteroepitaxial layer grown on the sapphire substrate misoriented by 5° toward the [0001] c-direction.[10] No cracks were observed. The brown color originates from infrared absorption due to nitrogen impurities. We want to emphasize that this wafer was obtained without the microneedle technique. Heteroepitaxial diamond wafer fabrication without the microneedle technique is much simpler and less costly.

We fabricated NO_2 p-type doped diamond MOSFETs on KENZAN Diamond™ with a 100-nm-thick Al_2O_3 passivation overlayer. The passivation overlayer increases the off-state breakdown voltage while ensuring a low drain leakage current. The MOSFETs were exhibiting a high drain current density and high breakdown voltage, demonstrating increased experimental BFOM and DC output power density due to the increased lateral breakdown field strength.

Figure 6 shows a schematic of the cross-section of the NO_2 p-typed doped heteroepitaxial diamond MOSFET with the Al_2O_3 passivation overlayer. The MOSFETs were fabricated on high-quality (001) KENZAN Diamond™ substrates. A 100-nm-thick diamond homoepitaxial layer was grown via microwave plasma chemical vapor deposition (MPCVD) on the KENZAN Diamond™. The microwave power was 750 W, and the working pressure was 50 Torr. CH_4 and H_2 source gases in a ratio of 1:100 were supplied during the growth.

H-diamond was exposed to 2% NO_2 diluted in N_2 to perform the NO_2 p-type doping. After NO_2 p-type doping, the H-diamond sample was immediately (within 15 mins) placed in metal evaporation chamber to ensure minimum desorption of NO_2 molecules prior to Au deposition. Then, a 50-nm-thick Au film was deposited as an ohmic contact. The region outside the Au-coated hole channel was isolated via O_3 exposure. Subsequently, a hole channel was created by

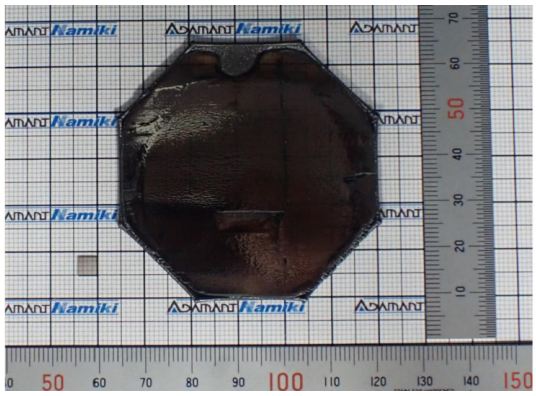

Fig. 5. Photograph of the 2 inch as-grown free-standing heteroepitaxial diamond wafer.[10]

separating the source and drain contacts through wet etching (KI/I_2).

During the formation of ohmic contacts, active channel underwent several processes which may have reduced the sheet concentration. To ensure p-type doping in the channel region, the channel was again exposed to NO_2 gas inside the atomic layer deposition (ALD) chamber, and without exposing it to the air, the channel was passivated with a 16-nm-thick Al_2O_3 bi-layer. The Al_2O_3 layers were deposited via ALD, where the sources of Al and O were trimethylaluminum (TMA) and H_2O, respectively. The first Al_2O_3 layer (4 nm thick) was deposited at 120 °C, and the second layer (12 nm thick) was deposited at 230 °C. This Al_2O_3 bilayer also functions as a gate-insulating layer.

A 50-nm-thick Au film was evaporated over the Al_2O_3 layer, and the gate was formed using a photolithography technique. Next, a 100-nm-thick Al_2O_3 passivation overlayer was deposited on the hole channel over the gate at 120 °C, as shown in **Fig. 6**.[11] The source-to-drain length (L_{SD}) was 15µm and the gate length (L_G) was 1.5 µm. The device characteristics were measured at 25 °C using a Keysight 1505A power device analyzer.

Figure 7(a) shows the DC output characteristics of the NO_2 p-typed doped heteroepitaxial diamond MOSFET with an Al_2O_3 passivation overlayer.[11] The MOSFET had a source-to-gate length (L_{GS}) and gate-to-drain length (L_{GD}) of 1.2 µm and 12.3µm, respectively. A gate bias (V_{GS}) of 9 V to −7 V was applied in steps of −1 V. The maximum I_D was measured to be −288 mA/mm at a V_{GS} of −7 V and drain voltage (V_{DS}) of −40 V. The on-resistance (R_{ON}) was estimated from the linear region of the I_D as 120 Ω· mm.

Fig. 7(b) shows the transfer characteristics of the MOSFET.[11] The threshold voltage (V_{th}) was determined to be 6.9 ± 0.1 V through linear extrapolation of the $\sqrt{I_D}$–V_{GS} characteristics. The current on/off ratio was $>10^7$. The gate leakage current (I_G) remained $<10^{-6}$ mA/mm, which is below the detection limit, and was thus negligible with respect to the drain currents. The transconductance (g_m) was obtained from the derivative of the transfer characteristics. The maximum g_m was estimated to be 29.63 mS/mm at V_{GS} = 0.72 V

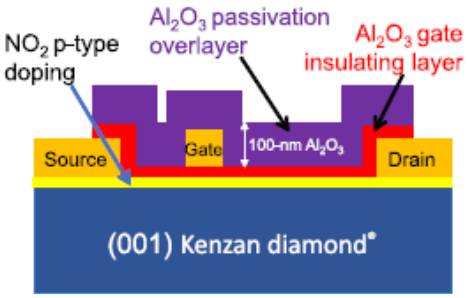

Fig. 6. Schematic of cross-section of NO_2 p-typed doped heteroepitaxial diamond (KENZAN Diamond™) MOSFET with an Al_2O_3 passivation overlayer.[11)]

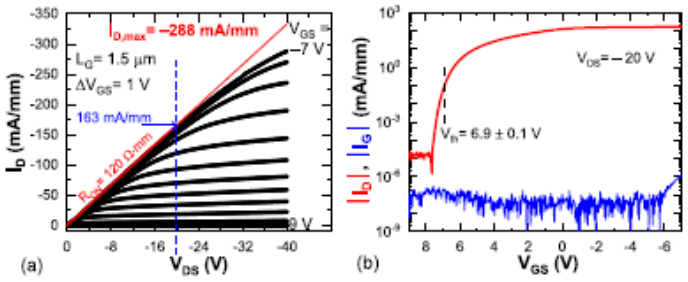

Fig. 7 (a) DC output characteristics and **(b)** transfer characteristics of NO_2 p-type doped MOSFET with Al_2O_3 passivation overlayer, fabricated on KENZAN Diamond™ .[11)]

The specific on-resistance ($R_{ON,spec}$) was determined to be 19.74 mΩ·cm^2 using the formula $R_{ON,spec} = R_{ON} \times (L_{SD} + 2L_T)$, where $2L_T$ is the contact transfer length of the source and drain and was reported as 1.45 µm. L_{SD} was 15 µm. R_{ON} of the respective MOSFET was described in Fig. 2(a). The BFOM was determined to be 344.6 MW/cm2 using the equation BFOM = $V_{BR}^2/R_{ON,spec}$, where V_{BR} = −2608 V. The obtained BFOM is the highest reported for any diamond MOSFET.

In conclusion, 2 inch diameter free-standing high-quality (001) diamond layers on misoriented (11$\bar{2}$0) A-plane sapphire substrates were grown in the step-flow mode. Using a misoriented substrate, the step-flow growth occurred and effectively decreased the tensile stress in the diamond. Consequently, without the microneedle technique, the natural delamination of the grown diamond layer from the substrate is possible. As the substrate misorientation angle increased, the XRC FWHM of diamond (004) and (311) diffractions decreased, thus the crystal quality improved. For diamond grown on a sapphire substrate with 7° misorientation toward the [1$\bar{1}$00] direction, the widths of the (004) and (311) XRC were 98.35 and 175.3 arcsec, respectively, which are the lowest ever reported. The curvature radius of diamond was 99.64 and 260.21 cm in the [1$\bar{1}$00] and [0001] direction of the substrate, respectively. The dislocation density was 2.6 × 10^7 cm^{-2}, and inclined dislocations were observed. This bunched-step structure proves that step-flow growth occurred on the diamond surface.

NO_2 p-type doped diamond MOSFETs were fabricated on KENZAN Diamond™ with a 100-nm-thick Al_2O_3 passivation overlayer. The MOSFETs showed the highest reported V_{BR} of −2608 V at an E_{BR} of 2 MV/cm. The MOSFET with L_G = 1.5 µm and L_{SD} = 15 µm, showed a maximum I_D of −288 mA/mm at a V_{DS} of −40 V. The $R_{ON,\,spec}$ of the device was estimated to be 19.74 mΩ ·cm^2. As a result, the MOSFET exhibited an experimental BFOM of 344.6 MW/cm^2. The passivation overlayer improved the high-voltage-endurance capability while ensuring a high I_D, which is essential for high power applications. Further, no degradation in on-state drain current was observed until V_{DS} = −500 V at V_{GS} = −1 V and sustained up to −1290 V. DC output power density was estimated to be 21.0 W/mm. Recently we demonstrated high performance of diamond MOSFET with modulation-doping.[12)]

We acknowledge Dr. Niloy Chandra Saha (Saga University) for his work and stimulating discussion.

REFERENCES

[1] R. J. Trew, J. B. Yan, and P. M. Mock, Proc. IEEE **79**, 598 (1991).
[2] A. Denisenko and E. Kohn, Diam. Relat. Mater. **14**, 491 (2005).
[3] Y. Yamamoto, T. Imai, K. Tanabe, T. Tsuno, Y. Kumazawa, andN. Fujimori, Diam. Relat. Mater. **6**, 1057 (1997).
[4] J. Isberg, J. Hammersberg, E. Johansson, T. Wikström, D. J. Twitchen, A. J. Whitehead, S. E. Coe, and G. A. Scarsbrook, Science **297**, 1670 (2002).
[5] M. Schreck, S. Gsell, R. Brescia, and M. Fischer, Sci. Rep. **7**, 44462 (2017).
[6] K. Ohtsuka, K. Suzuki, A. Sawabe, and T. Inuzuka, Jpn. J. Appl. Phys. **35**, L1072 (1996).
[7] H. Aida, S.-W. Kim, K. Ikejiri, Y. Kawamata, K. Koyama, H. Kodama, and A. Sawabe, Appl. Phys. Express **9**, 035504 (2016).
[8] S.–W. Kim, Y. Kawamata, R. Takaya, K. Koyama, and M. Kasu, Appl. Phys. Lett. **117**, 202102 (2020).
[9] S. Yugo, T. Kanai, T. Kimura, and T. Muto, Appl. Phys. Lett. **58**, 1036 (1991).
[10] S. –W. Kim, R. Takaya, S. Hirano, and M. Kasu, Appl. Phys. Express **14**, 115501 (2021).
[11] N. C. Saha, S. –W. Kim, T. Oishi, Y. Kawamata, K. Koyama, and M. Kasu, IEEE Electron Dev. Lett. **42**, 903-906 (2021).
[12] M. Kasu, N. C. Saha, T. Oishi, and S. –W. Kim, Appl. Phys. Express 14, 051004 (2021).